Journal Pre-proof

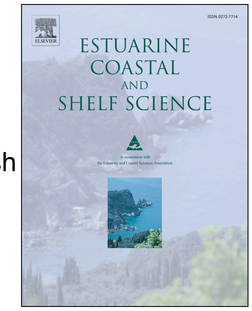

River plume and sediment transport seasonality in a non-tidal semi-enclosed brackish water estuary of the Baltic Sea

J. Salmela, E. Kasvi, P. Alho

PII: S0272-7714(20)30717-4

DOI: https://doi.org/10.1016/j.ecss.2020.106986

Reference: YECSS 106986

To appear in: *Estuarine, Coastal and Shelf Science*

Received Date: 17 April 2020

Revised Date: 19 August 2020

Accepted Date: 25 August 2020

Please cite this article as: Salmela, J., Kasvi, E., Alho, P., River plume and sediment transport seasonality in a non-tidal semi-enclosed brackish water estuary of the Baltic Sea, *Estuarine, Coastal and Shelf Science* (2020), doi: https://doi.org/10.1016/j.ecss.2020.106986.

Author contributions - CRediT author statement

Jouni Salmela: Conceptualization, Methodology, Formal Analysis, Investigation, Writing – Original Draft, Visualization, Project Administration, Funding Acquisition

Elina Kasvi: Conceptualization, Investigation, Writing – Review & Editing, Visualization, Supervision, Funding Acquisition

Petteri Alho: Conceptualization, Writing – Review & Editing, Visualization, Supervision, Funding Acquisition

River plume and sediment transport seasonality in a non-tidal semi-enclosed brackish water estuary of the Baltic Sea

J. Salmela[1*], E. Kasvi[1,2], P. Alho[1,3]

1. University of Turku, Department of Geography and Geology, FI-20014, Turun yliopisto, Finland, jouni.jsalmela@utu.fi (*corresponding author)
2. Turku university of Applied Sciences, Joukahaisenkatu 3, FI-20520, Turku, Finland
3. Finnish Geospatial Research Institute, Geodeetinrinne 2, FI-02430, Masala, Finland

Abstract

Our study aims to determine the development of sediment-rich freshwater plumes in a non-tidal brackish water-dominated (salinity < 6) estuary in the Halikonlahti Bay, Northern Baltic Sea. We studied three seasons with different wind conditions and discharges: two open water periods, one with low (~ 0.2 m³/s) and one with high (31 – 40 m³/s) river discharges, and one ice-covered period with high (28 – 40 m³/s) river discharge. To conduct our analyses, we measured suspended sediment concentration (SSC), turbidity, salinity and temperature of bottom and surface waters together with current measurements along the estuary. Water samples were collected with LIMNOS water sampler and current measurements were done with acoustic Doppler current profiler. The results indicate that river plume develops under high river discharge, while during low river discharge the plume is very limited in extent. In open water conditions, SSC increased approximately ten-fold in the estuary head, with increased discharge from 0.2 m³/s to 31 m³/s. Buoyant plumes developed in both open channel and ice-cover conditions during high river discharge periods even in a weakly stratified environment, where the salinity difference was less than five over the entire water column. Unlike salinity, small temperature differences between river and seawater did not contribute the development of buoyant sediment plume. Weak stratification together with reduced wind-induced mixing was found to limit the sediment mixing between fresh surface and saline (~ 5) bottom layers in both ice-covered and open water conditions. For example, even 2 – 5 times higher SSCs were found at surface waters compared to bottom waters over a shallow (~ 4 m) water column. Wind and river discharge induced estuarine currents were found. Inverse estuary circulation developed under the conditions of low river discharge and inshore directed wind. High river discharge together with salinity stratification formed a positive estuarine circulation pattern, with surface outflow and bottom inflow.

Keywords: River plume, sediment transport, stratification, under-ice plume, current measurement, Baltic Sea, Archipelago Sea

1 Introduction

River plumes can contribute positively or negatively to estuarine environments and have a strong impact on water quality and biological productivity. Sediment- and nutrient-rich freshwater enables fish habitats (Cyrus and Blaber, 1992; Gilbert et al., 1992), maintains delta areas (Coleman, 1988), reduces light penetration and thus affects primary production (Pedersen et al., 2012). Sediment transport is also associated with pollutants (Yuan and Yang, 2001; Fernandez et al., 2017) and the particulate nutrients, such as nitrogen and phosphorus (Beusen et al., 2005), which in turn cause eutrophication (HELCOM, 2009). For fragile sea areas especially, such as the Baltic Sea, eutrophication is one of the biggest environmental alterations of recent centuries, partly due to nutrient-rich runoff (Hänninen et al., 2000; Bonsdorff et al., 2002). It is therefore important to understand the factors affecting river plumes and their seasonal behaviour.

The behaviour of river plumes has been found to be consistent with the combination of freshwater flows and tidal ranges. Plumes may be occasional or persistent, depending on tide and discharge magnitude (Walker et al., 2005; Pritchard and Huntley, 2006). In non- or micro-tidal estuaries, river plumes may not exist or may be located inshore at low river discharges, while at high river discharges river plumes extend further offshore (Granskog et al., 2005a; Restrepo et al., 2018). Variations in a tidal range influence plume development and sediment transport, that results from tidal pumping, during flood tides, saline seawater inflows, while during ebb tides, saline seawater outflows (Stumpf et al., 1993). This tidal pumping may cause sediment resuspension and, therefore, higher SSC in the water column (Grabemann et al., 1997; Wu et al., 2012). Numerous studies have focused on determining the development and location of higher SSC, also known as the estuary turbidity maxima zone (ETMZ), where suspended sediments are trapped and turbidity is at its highest. ETMZs are highly mobile and located between freshwater-saline fronts in response to the changing freshwater flows and tidal ranges (Hir et al., 2001; Uncles et al., 2006; Chen et al., 2015; Mitchell et al., 2017; Restrepo et al., 2018). However, some seas, such as the Mediterranean Sea and the Baltic Sea, have very weak tides and lack tidal pumping. Thus, the behaviour of sediment-rich river plumes in non-tidal areas requires more attention.

In addition to tidal influence, saline-induced stratification (halocline) influences river plume behaviour and sediment transport, separating estuarine water into two distinct horizontal layers: buoyant freshwater and saline bottom water (Granskog et al., 2005a; Ren and Wu, 2014; Kari et al., 2018; Restrepo et al., 2018). The halocline may prevent sediment mixing between the two water layers (Stumpf et al., 1993) and create a zone of higher sediment concentration (Ren and Wu, 2014). However, a water column may become vertically mixed by wind stress or tidal influence, leading to sediment mixing between the layers (Stumpf et al., 1993; Xia et al., 2007; MacCready et al. 2009). The behaviour, shape and size of the river plume may be also driven by wind stress at the water surface (Kourafalou, 2001; Molleri et al., 2010). Despite the importance of the halocline, only few studies have focused on saline-induced stratification in brackish water estuaries (Granskog et al., 2005a; Granskog et al., 2005b; Kari et al., 2018), where salinity is much lower than in oceans. These studies stated that freshwater from rivers forms an under-ice plume due to both saline or density differences between buoyant freshwater and underlying seawater and the lack of wind-induced mixing due to ice cover. Granskog et al. (2005a) found also small river plume during open water conditions.

Estuary studies have successfully contributed to understanding the seasonal variation in sediment plume behaviour and development in open water (Van Maren and Hoekstra, 2004; Wu et al., 2012). While Van Maren and Hoekstra (2004) found that the salinity stratification in a shallow microtidal tropical estuary is strongly season-dependant, Wu et al. (2012) stated that turbidity maxima in mesotidal estuary is strongly seasonal in magnitude and extent. However, comparative studies of sediment transport under different seasonal and flow conditions at high latitude zones, where the ice cover may affect estuary conditions, are sparse. Only a few studies have contributed to knowledge of the effect of an ice cover on freshwater plumes (eg. Ingram and Larouche, 1987; Granskog et al., 2005a and 2005b; Kari et al., 2018). They all found that buoyant river plumes develop in ice-cover conditions mainly due to reduced wind induced mixing and stratified water column. Ice-cover may also restrict the horizontal extent of river plumes (Macdonald and Carmack, 1991; Kuzyk et al., 2008). These studies have shown that large-scale under-ice topographies (ridges) along the boundary between landfast ice and pack ice both restrict the horizontal extent of river plumes, containing it within a certain area, and have an influence on under-ice surface salinity and stratification. In addition, the timing of spring freshet in relation to ice-cover breakup also influences on the plume extent (Ingram et al. 1996). However, these studies did not focus on SSC or sediment mixing between fresh river water and saline seawater. While most studies of sediment transport have been undertaken in tidal, saline estuaries, such studies in non-tidal, brackish water environments are lacking. In particular, the role of stratification and estuarine currents in sediment transport in brackish water estuaries deserves more attention.

Our aim is to understand how the behaviour of river plumes, and thus sediment transport, is controlled by seasonal variation of river discharge and sea ice cover in a semi-enclosed non-tidal brackish estuary. Here, non-tidal brackish estuary is defined as an estuary at the freshwater-brackish water interface. We also study the effects of stratification and wind on the river plumes. We assume that 1) river discharge variation controls plume development and sediment transport and 2) even a low saline difference between fresh- and seawater maintains the stratification and development of buoyant river plumes. We test these assumptions by combining measurements on horizontal and vertical variation of current and water quality with river discharge and wind monitoring data during different seasons in the Archipelago Sea (AS), Baltic Sea. Our data covers two open water periods including low and high river discharges and one ice-cover period with high river discharge.

2 Study area

Halikonlahti Bay is located on the coast of south-western Finland at the AS, Baltic Sea (Fig. 1). Our study area is located in the inner archipelago, where Kemiönsaari Island divides Halikonlahti Bay into northern and southern channels. The height of Kemiönsaari Island is relatively low with the highest point approximately at 68 meters above sea level. Both channels are 250–2000 m in width and more than 40 km long (the distance between the river mouth and open sea). Channel depths vary between 30 m and < 3 m sections, with an average depth of 12 m along the thalweg (Fig. 1). In particular, the southern channel has a very shallow sill that restrict water exchange between the open sea and the channel. Relatively steep banks and gently sloping fields surround both channels. The channels are non-tidal (tidal range < 0.03 m) and brackish with salinity between 2 and 6. The Uskelanjoki and Halikonjoki rivers flow into the bay, together forming the main freshwater inflow into the estuary. The discharge of the Uskelanjoki River has been monitored since 1970, with a long-term (1971–2018) mean annual discharge of only 4.9 m^3/s, while daily peak river discharge is up to 140 m^3/s. Peak discharges occur mainly during spring due to snowmelt, but they may also occur occasionally throughout the year. During snowmelt period the bay may be either ice-covered or ice-free. In this study, the discharge of the Uskelanjoki River was used to represent discharge into the estuary. The total catchment area for these two main rivers is 873 km^2: 307 km^2 for the Halikonjoki River and 566 km^2 for the Uskelanjoki River. The catchment area is heavily cultivated, 36% non-irrigated arable land based on CORINE Land Cover classification. The bay and the rivers are typically ice-covered between late December and mid-March, except for a few narrow inlets that might stay open during winters due to sea currents.

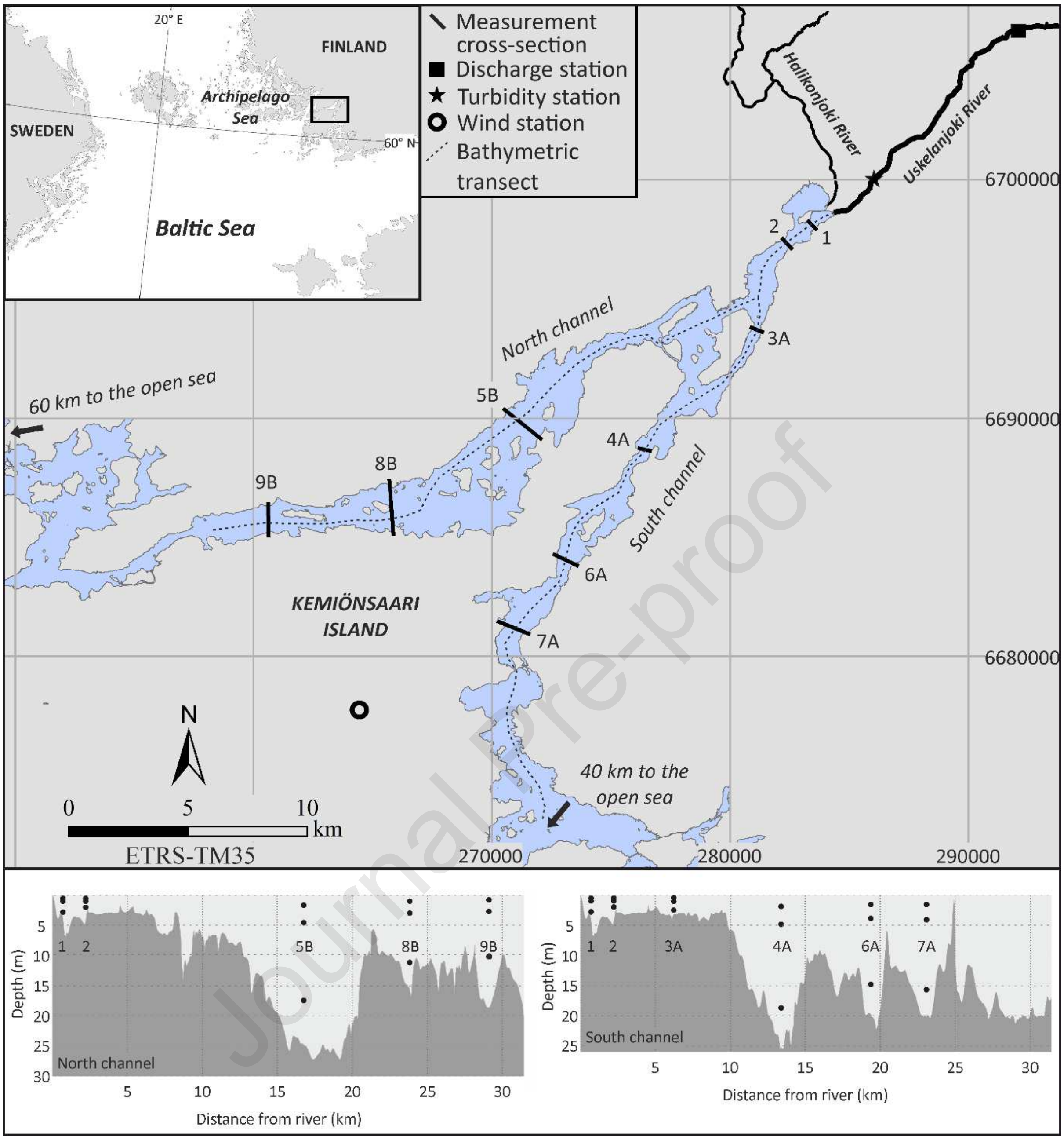

Figure 1. The study area and the locations of measurement cross-sections 1 – 9B and water samples. Halikonlahti Bay consists of two channels that connect the bay to the open sea. Letters A and B in the cross-section name refer to the south and north channels, respectively. Vertical location of the water samples at south and north channels are shown in the bathymetric transects. Each water sample depth was related to the measured water depth of the measurement site. The bathymetric transects are based on Coastal Terrain Model of the Archipelago Sea produced by Department of Geography and Geology, university of Turku.

The Baltic Sea is a shallow brackish water (surface salinity between 2 and 8) sea where the gradient is relatively stable. In the AS the surface salinity ranges between 2 and 5. The AS consist of thousands islands and inlets and the shallowness and number of islands restrict efficient water exchange between the narrow bays, straits and the open sea (Erkkilä and Kalliola, 2004). The AS is characterized by both a halocline and a seasonal thermocline. While the halocline is stable, the thermocline occurs only during summers due to the solar heating of surface water. Both clines isolate the surface layer from the well-mixed uniformly saline bottom layer. While the halocline is located typically between the depths of 40 m and 80 m (Fonselius, 1969), the thermocline is located between the depths of 15 m and 20 m (Kullenberg and Jacobsen, 1981). We do not expect to find a halocline in our study area because the deepest area is shallower than 30 m. However, temperature and salinity differences between freshwater and saline seawater may cause local vertical stratification.

3 Material and Methods

We performed three field campaigns – summer 2018 (S18), winter 2019 (W19) and autumn 2019 (A19) – during which data of current velocity and direction, water quality and Secchi depth were collected in both horizontal and vertical dimensions in the estuary (Table 1). In addition, we derived data of the daily river discharge and turbidity of the Uskelanjoki River from the Finnish Environment Institute (SYKE) and Economic Development, Transport and the Environment Centre (ELY), respectively, and wind data of Kemiönsaari weather station from the Finnish Meteorological Institute (FMI).

Table 1. Details of the data used in this study.

	S18 (Summer 2018)		W19 (Winter 2019)		A19 (Autumn 2019)	
Condition	Open water		Ice cover		Open water	
Date	27/6	28/6	20/3	21/3	14/11	15/11
Channel	North (B)	South (A)	North (B)	South (A)	North (B)	South (A)
Number of water quality measurements	12	19	15	15	18	30
Water sampling depth (% of the site depth)	20/80	20/80	10/20/80	10/20/80	10/20/80	10/20/80
Number of flow measurements	6	9	5	5	6	9
River discharge	-- Derived from SYKE --					
River turbidity	-- Derived from ELY --					
Wind direction and speed	-- Derived from FMI --					

3.1 River discharge, turbidity and wind data

The Uskelanjoki River discharge gauging station (Kaukolankoski, 2500400), located ca. 13 km upstream from the river mouth, monitors daily river discharge variation. Kaukolankoski covers 85 % of the total catchment area of Uskelanjoki River. We derived river discharge data, provided by SYKE, to create a hydrograph for years 2018–2019 (Fig. 2). To evaluate the water turbidity (NTU) of the freshwater flow entering the estuary, we used the turbidity data derived from ELY's continuous water quality gauging station, where turbidity was measured with Scan Nitrolyser spectrometer. These turbidity measurements are not directly comparable to turbidity measurements conducted along the estuary and they represent only the variation with time and discharge. The station is located 2.6 km upstream from the river mouth. Daily turbidity averages were calculated based on 30 min measurement intervals.

Wind data, provided by FMI, was derived from the national weather station (Kemiönsaari Kemiö, 100951) located on Kemiönsaari Island (Fig. 1). The weather station is located in an open field approximately 10 meters above sea level within 4 and 7 km distance to the south and north channels respectively. The station provides 1h interval wind data. Variation of wind direction and speed was calculated separately for each field campaign days (Table 2) and for the period one week prior to the field campaigns (including field campaign days) (Fig. 3).

3.2 Water quality

To evaluate the extent of multiple river plumes, water samples were collected at 10%, 20% and 80% (hereafter 0.1, 0.2 and 0.8) of the site depth (except during S18 – 0.2 and 0.8 only) on the left and right sides of the channels coincident with current measurements. Samples of 500 ml or 1 000 ml were collected with a LIMNOS water sampler. We focused on four different water quality parameters: turbidity, SSC, temperature and salinity. While temperature was measured in the field, other parameters were measured at the laboratory. Turbidity (NTU) was measured using an Analite NEP160 turbidity sensor and water temperature (accuracy ±0.2°C (YSI, 2020)) and salinity (accuracy ±1.0% of reading or ±0.1 ppt (YSI 2020)) using a YSI Professional Plus water quality meter. Salinity was measured using Practical Salinity Scale. To evaluate SSC the water samples were filtered using filters with pore sizes 0.7 μm and 0.45 μm. First, water samples (based on turbidity) were filtered through 0.7 μm filter and later 100 ml of filtered water were refiltered through 0.45 μm filter. Both filters were dried in 105 °C for 2 hours to determine the dry weight. Organic matter was removed from the 0.7 μm filter by loss on ignition (LOI). We also conducted Secchi depth measurements using white 0.3 m circular disc at each site during the open water periods to evaluate the dispersion of the river plumes. We averaged the water quality data and the Secchi depths for each CS using the values from both the right and left sides. Thus, we had one value for each depth from each measurement CS.

3.3 Current measurements

To evaluate the vertical structure of the sea currents along the estuary, we conducted 6 min stationary measurements, with a sample measurement frequency of 1 Hz, using an acoustic Doppler current profiler (ADCP) (Sontek, M9). The measurements were performed during low and high river discharge periods, two open water conditions and one ice-cover condition (Table 1). In total, nine measurement cross-sections (CSs) were selected based on the water depth and the distance from the river mouth (Fig. 1). At each CS (except CS 2), the current was measured on both the left and right sides of the channel. For open water measurements (S18 and A19), the ADCP was mounted on a raft attached to the stern of an anchored boat. During ice cover (W19), the sensor was hand held and levelled below the ice cover. While in open water measurements, the transducer depth was set to standard 0.11 m, for ice-cover measurements, the depth of 0.4 m was used due to the thickness of the ice cover. The partly melted ice cover in both channels during W19 restricted us from measuring at all nine cross-sections.

The current data was post-processed and corrected based on magnetic declination and mean water temperature and salinity at each site. To evaluate inflow and outflow, the current data was cross-sectional oriented – the velocity and direction were related to the direction of the CS (see Fig. 1 for CSs). We evaluated the cross-sectional direction (perpendicular to the channel) of each measurement and calculated the along-channel velocity. Final data consisted of current direction – either positive (outflow) or negative (inflow) – and velocity profile for each measurement. Due to the ADCP's capability to adjust the measured cell height in relation to water depth, the cell height varied between the measurements from 0.06 m to 2.00 m.

4 Results

4.1 River discharge and turbidity in the Uskelanjoki River

Our first field campaign (S18) took place during a low river discharge and turbidity period, when the discharge of the Uskelanjoki River was approximately 0.2 m³/s (Fig. 2 Table 2). A low river discharge period of approximately 36 days preceded S18 campaign. The last higher flow event (26.5 m³/s) was recorded on the 2nd of May, 56 days before S18. Similarly, the turbidity was low (33 NTU) during S18, and turbidity remained low (< 50 NTU) for 21 days before S18. The second field campaign (W19) took place at a river discharge of 27–39 m³/s and turbidity of 287–353 NTU. The turbidity of the river was approximately 10 times higher than during S18. W19 took place during the peak flow of a snowmelt-induced discharge period (Q > 10 m³/s) that started four days before W19. River turbidity remained above 100 NTU during the last 11 days before our field campaign. The third field campaign (A19) took place during a high discharge period in autumn, caused by heavy rainfall. River discharge was 31–40 m³/s and turbidity was 499–584 NTU during the two-day field campaign. River turbidity during A19 was highest among the three measurement periods and was nearly 15 times higher than during S18. River discharge was still low (< 1 m³/s) on the 9th of November, only five days before the peak discharge on the 14th of November.

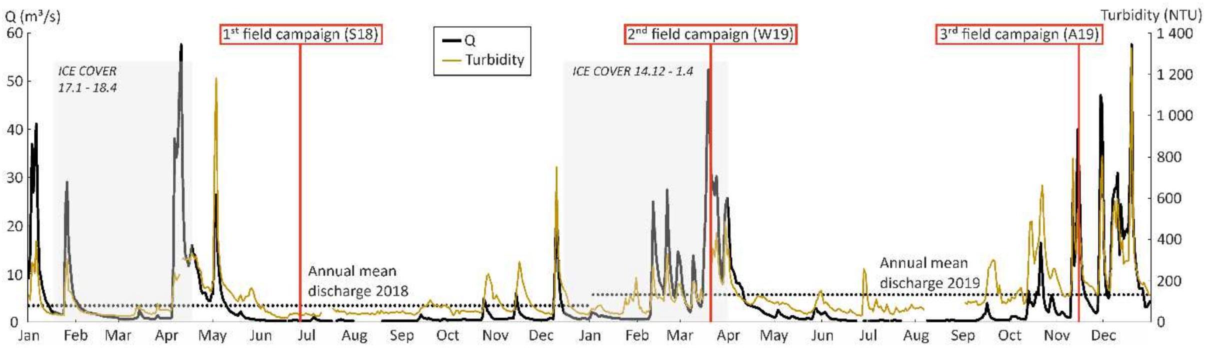

Figure 2. Hydrograph and turbidity variation of the Uskelanjoki River for the two-year study period. Shaded area illustrates the length of the ice-cover period in Halikonlahti Bay.

4.2 Wind, salinity and temperature

During S18 campaign, the average wind direction was towards the river mouth, parallel with both channels. The wind speed was higher on the second day (south channel) than on the first day (north channel), with moderate and gentle breeze, respectively (Table 2). Wind conditions one week prior to the campaign were stable and mainly towards river mouth parallel with both channels (between 180 and 270 degrees) (Fig. 3). Wind speed remained below 10 m/s and the highest wind speed (8.6 m/s) was recorded on 22nd of June, five days before the field campaign. During S18, the salinity remained constant between the surface and bottom up to 13 km from the river mouth, where the bottom became about 0.5–1.0 saltier than the surface (Fig. 4). Salinity was lowest (2.1) closest to the river mouth and increased steadily towards the sea, being highest (4.5–5.0) at the furthest CS. The temperature difference between the surface and bottom was highest (more than 10 °C) at the deepest CSs. The surface temperature difference between inshore and offshore CSs was 3.3 °C.

Table 2. River discharge and turbidity with wind direction and speed variation during the field campaigns.

	S18		W19		A19	
Date	27.6	28.6	20.3	21.3	14.11	15.11
Channel	North (B)	South (A)	North (B)	South (A)	North (B)	South (A)
Daily river discharge (m^3/s)	0.23	0.2	39.5	27.5	40	31.2
Daily river turbidity (NTU)	33	33	353	287	548	499
Wind direction (deg)	227–277	213–247	206–257	177–244	174–178	11–112
Wind speed (m/s)	3.4–4.3	5.5–8.8	3.8–8.0	2.9–6.2	7.5–8.3	1.7–2.1

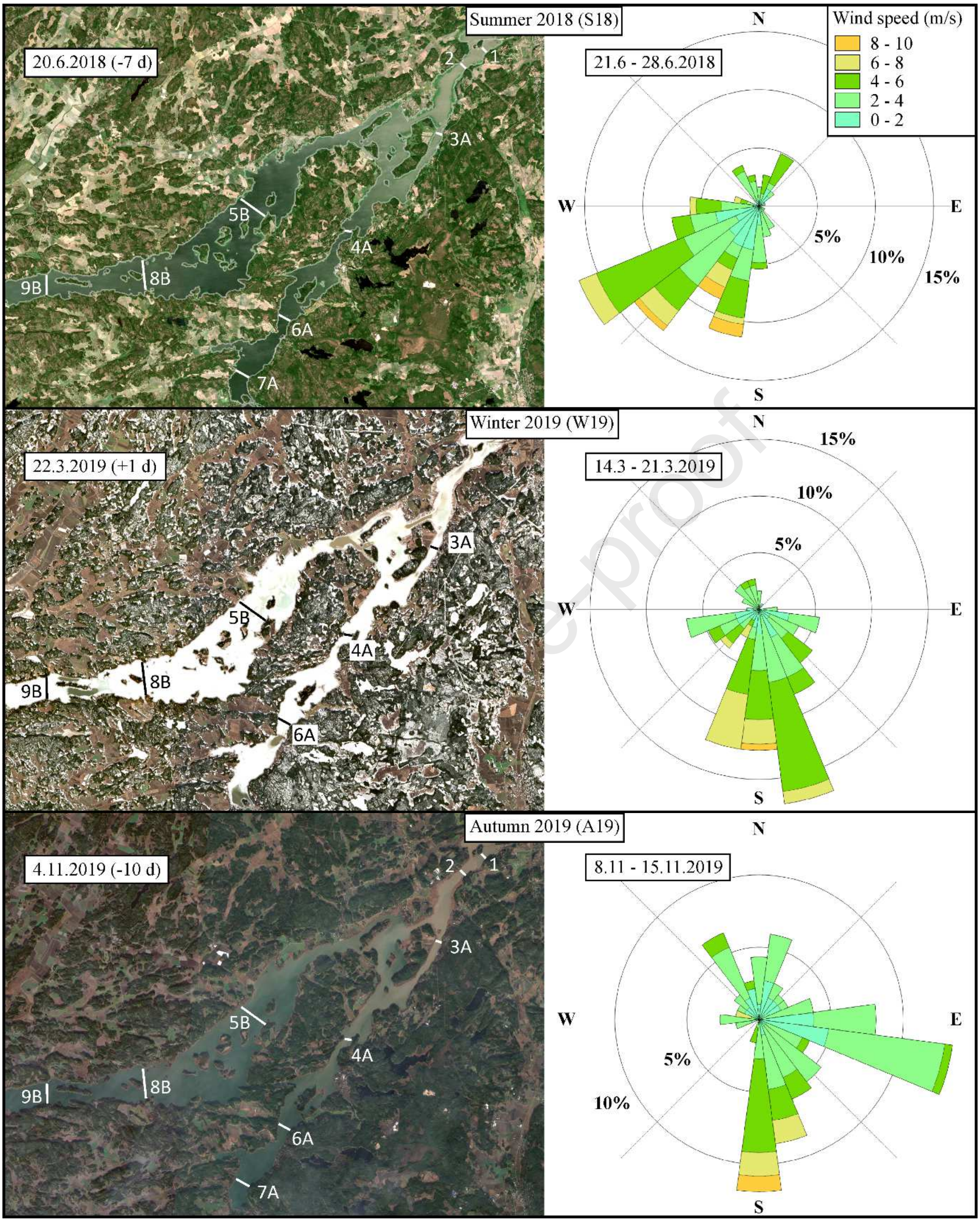

Figure 3. True colour Sentinel 2 satellite images and wind roses from the study area. Cloudless satellite data were available for summer, winter and autumn 7 days before, 1 day after and 10 days before field campaigns respectively. Wind roses show the data for a one-week period prior to the field campaigns (including the field campaign days).

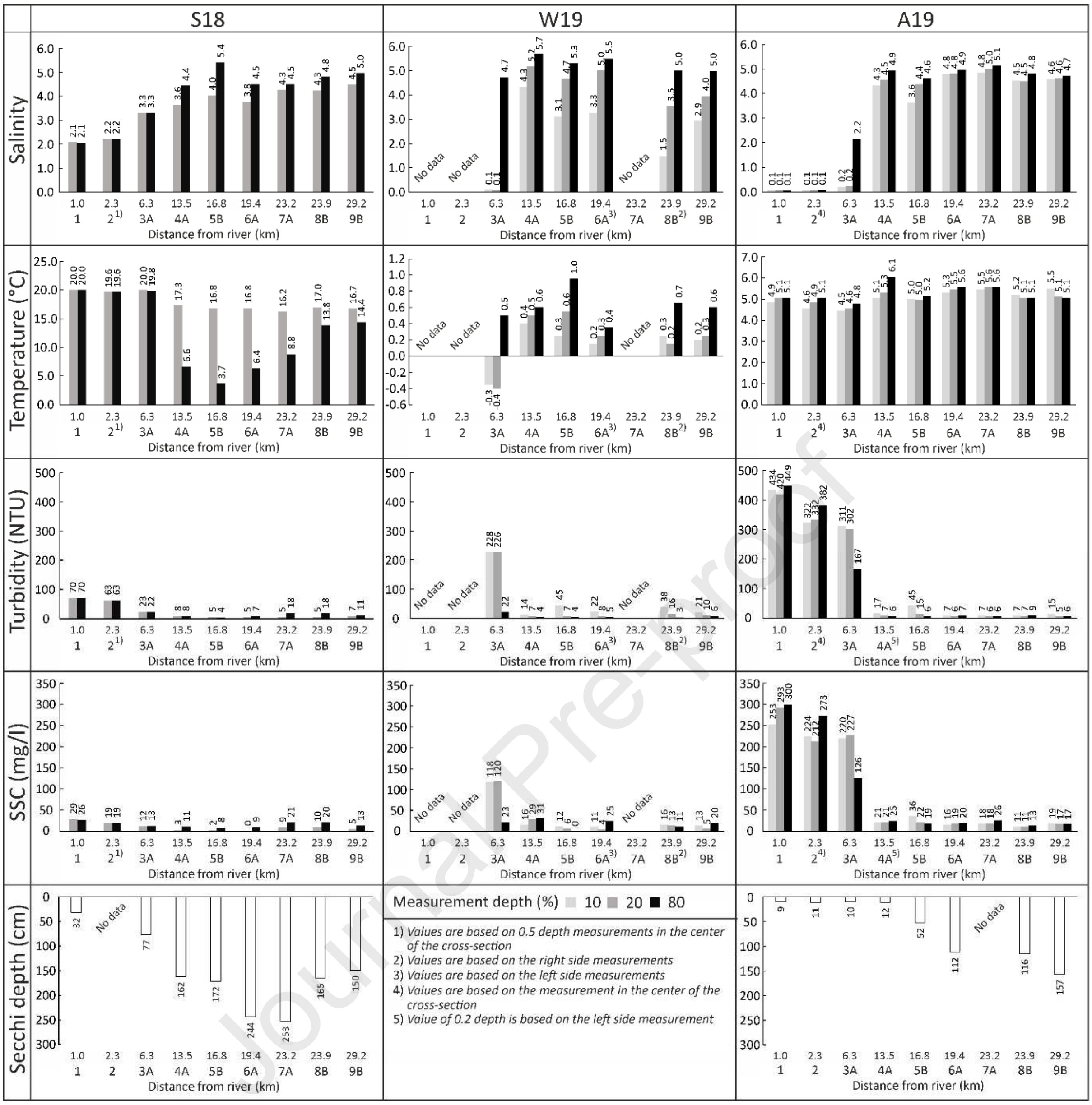

Figure 4. Salinity, temperature, turbidity and SSC of the water samples and Secchi depths at measurement cross-sections. X-label of each graph shows both the distance from the river and the cross-section name. Letters A and B in the cross-section name refer to the south and north channels, respectively.

During W19 (high discharge and ice cover), the wind direction was similar to S18, once again parallel with both channels. The variation in wind direction was small between the days, and the wind speed showed similar values, between gentle and moderate wind. Southerly winds prevailed one week prior to the field campaign. Like in S18, the wind speed remained below 10 m/s and the highest wind speed (9.6 m/s) was recorded on 17th of March, three days before the field campaign. The highest salinity difference (4.6) between the surface and bottom located at CS 3A, where the surface salinity was only 0.1, while the bottom salinity was 4.7. The surface was less saline throughout the estuary, and the salinity difference between 0.1 and 0.8 depths varied between 1.4 and 4.6. The surface salinity did change from CS 4A seawards, while the bottom salinity remained relatively constant. Unlike salinity, the temperature measurements showed a great homogeneity of the water column, having differences between the surface and bottom layers less than 1 °C throughout the estuary.

Unlike S18 and W19, during A19, the wind direction was not parallel to the channels during the campaign. There was constant moderate southerly winds during the first day at the north channel. This average wind speed (7.5 – 8.3 m/s) was the highest of all field campaigns and partly perpendicular to the north channel (from left to right when looking offshore). During the second day, the variation of wind direction was biggest, between 11 and 112 degrees, but mainly towards offshore. However, the wind was light (e.g. no waves) and not expected to influence water movement. Wind direction was mainly between south and east one week prior to the field campaign. Variation in wind direction one week prior to the campaign was strongest during A19, when constant 2 – 6 m/s northerly winds were also recorded. Once again, wind speed did not exceed 10 m/s one week prior to field campaign. The highest wind speed (6.5 m/s) was recorded on 12th of November, two days before the first field campaign. The salinity was the same at the estuary head (CS 1–2) at surface and bottom. At CS 3A, the salinity difference between the bottom and surface increased, being 2.2 and 0.2, respectively. From CS 4A seawards, the water salinity became more uniform within the water column. The surface and bottom salinity difference became less than 1.0. Based on temperature data, the estuary water was both vertically and horizontally homogeneous, having a temperature variation of ~1 °C along the whole study area.

4.3 Current direction and velocity

During S18, the surface current was mainly towards the river mouth (inflow) and the bottom current towards the sea (outflow) (Figs. 5–6; highlight I–II). At CS 1, there was an inflow in the whole water column at a speed of 0.01–0.05 m/s, being highest at the surface. The strongest current velocity appeared at the west side of CS 3A, where the surface inflow exceeded 0.1 m/s. This location and CS

1 were the only ones where there was inflow in whole water column; in the rest of the CSs, the surface and bottom layers flowed in opposite directions. In the north channel, the surface water inflow was between 0.00 and 0.09 m/s, while the bottom outflow was slightly higher (0.00–0.13 m/s). The boundary between these two layers was located approximately at a depth of 2–4 m. A similar boundary was located at the same depth in the south channel, where the velocity of the surface inflow was highest (0.13 m/s), but mostly between 0.00 and 0.06 m/s, which was slightly smaller than in the north channel. Simultaneously, the bottom outflow had a speed of 0.00–0.06 m/s. The velocity of the surface and bottom layers did not change with distance to the river mouth.

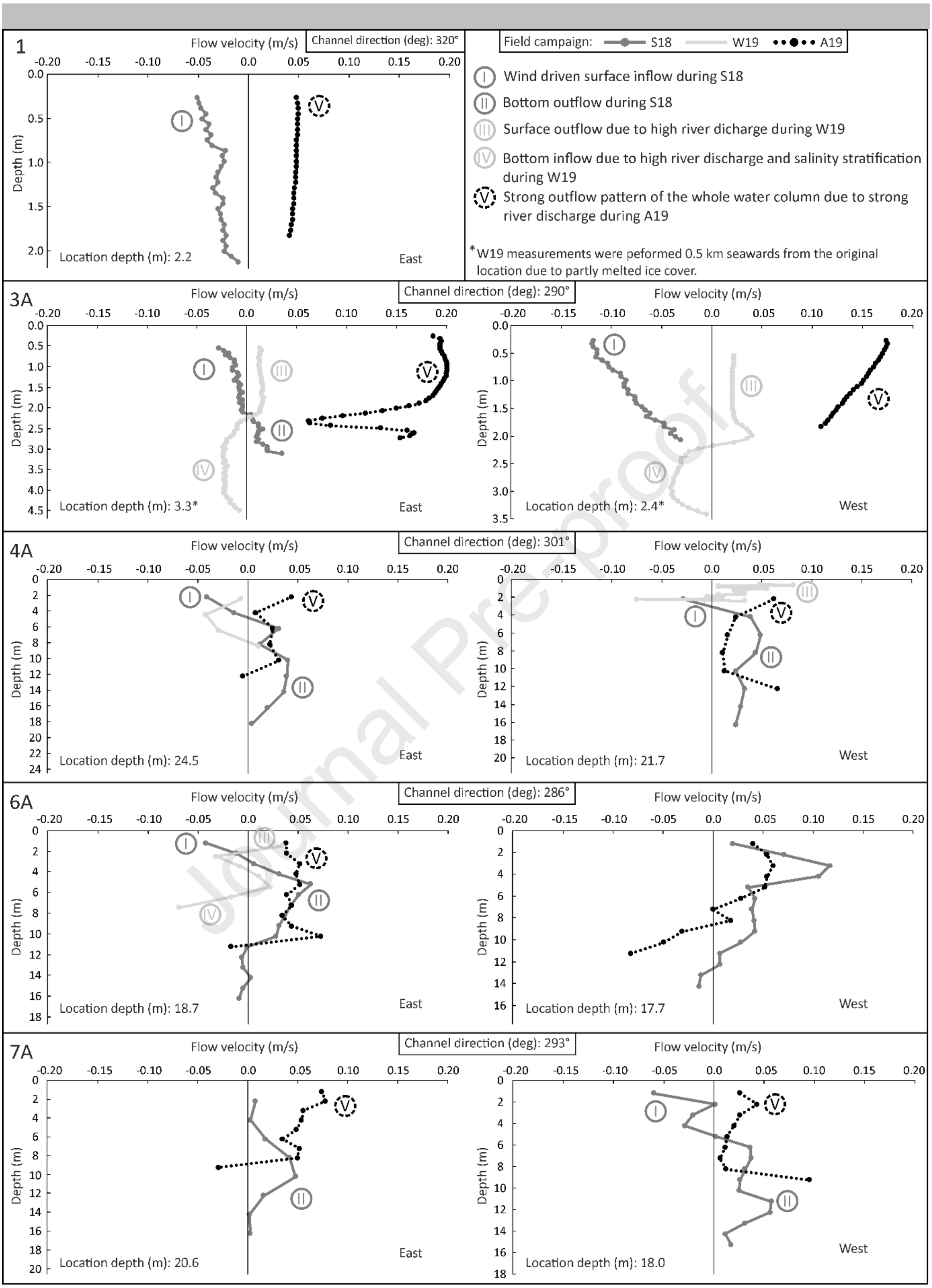

Figure 5. Current direction and velocity in the south channel during the three different field campaigns. Negative values indicate inflow and positive values outflow. Cross-sections 3A–7A have

east and west measurement sides. Channel directions indicate the main channel direction in the outflow direction. Highlighted features I–V are discussed in the text.

The circulation pattern during W19 was opposite to that of S18. During W19 surface outflowed and bottom inflowed (Figs. 5–6; highlights III–IV). Outflow was found at each CS that we were able to measure during the ice cover period. The surface outflow velocity varied between 0.00 and 0.08 m/s along the estuary, being highest (0.08 m/s) at the west side of CS 4A. Bottom inflow was not as clear as surface outflow, but it was clearly seen especially at CS 3A, where the whole surface layer (depth less than 2.2 m) outflowed and bottom layer inflowed steadily. Both surface and bottom layer velocities varied between 0.00 and 0.04 m/s.

The highest current velocities during the study period were measured during A19, when strong outflow was located at each CS (Figs. 5–6; highlight V). The outflow covered nearly the whole water column at many CSs, contrary to S18 and W19. The strongest outflow velocity 0.15–0.2 m/s was located at surface (depth less than 1 m) at CS 3A. At the rest of the CSs, the outflow velocity varied between 0.00 and 0.08 m/s. At the estuary head (CS 1), the outflow velocity remained between 0.04 and 0.05 m/s, which was less than in CS 3A. However, the whole water column (depth of 2 m) outflowed at a similar velocity between CSs 1 and 3A. The surface velocities were slightly higher in the south channel than in the north channel.

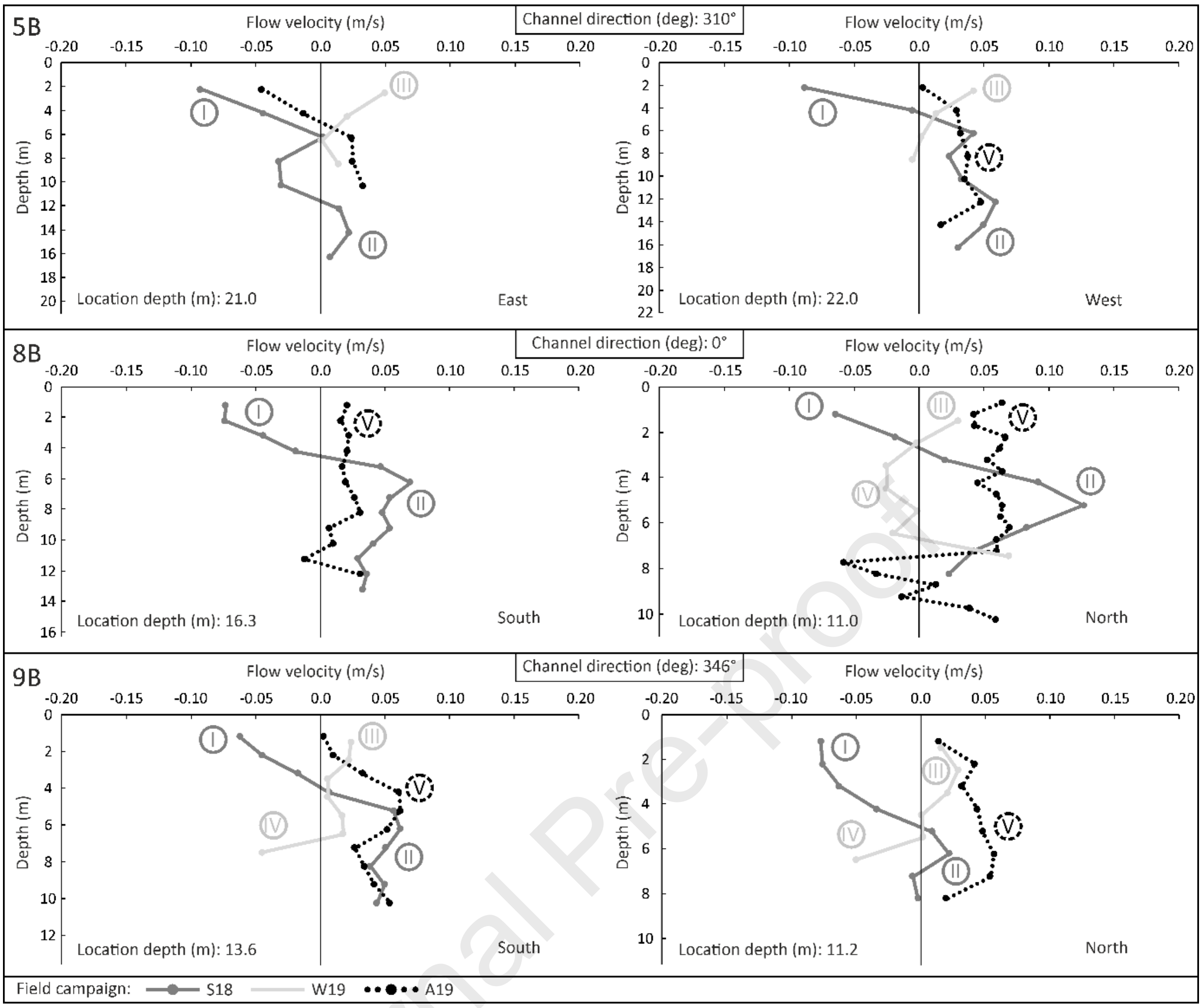

Figure 6. Current direction and velocity in the north channel during the three different field campaigns. Negative values indicate inflow and positive values outflow. Each cross-sections 3A–7A have east/south and west/north measurement sides. Channel directions indicate the main channel direction in the outflow direction. Highlighted areas I–V are described in Figure 5 and discussed in the text.

4.4 Turbidity, SSC and Secchi depth

During S18, the turbidity was similar between the surface (0.2 depth) and bottom (0.8 depth), all the way to 20 km from the river mouth (CS 6A). This indicates the homogeneity of the water column. The highest turbidity, 70 NTU, was located closest to the river mouth at CS 1. Between CSs 2 and 3A, within 4 km, the turbidity dropped from 62 to 23 NTU and remained mainly below 20 NTU from the CS 3A seawards. The SSC showed a similar trend to that of turbidity (correlation 0.82) (Table 3) having the highest values (26–29 mg/l) closest to the river mouth. The SSC declined steadily towards the sea, being 5 and 13 mg/l 0.2 and 0.8 depths, respectively, closest to the open sea. From CS 4A (13.5 km) seawards, the SSC at the bottom became clearly higher than at the surface. Secchi depth measurements showed similar trend with surface SSC, increasing seawards, being the lowest (32 cm) at CS 1 and the highest (253 cm) at CS 7A.

During W19, the highest turbidity values were at CS 3A, the closest CS to the river mouth we were able to measure due to deteriorated ice in the estuary. At CS 3A, the surface turbidity (226 NTU) at 0.2 depth was 10 times higher while the bottom turbidity (22 NTU) was similar to during S18. While the highest turbidity values were measured at 0.1 depths, the smallest were at 0.8 depths at every CS. The surface turbidity decreased seawards, especially between CSs 3A and 4A, where the turbidity of 0.1 depth dropped from 228 to 14 NTU within 7 km. Meanwhile, the bottom turbidity dropped from 22 to only 4 NTU. The SSC was highest once again at the same CS (3A) as the turbidity (Fig. 4). Turbidity and SSC showed very strong correlation (0.95) and similar pattern along the estuary in W19 (Table 3). While the surface (0.2 depth) SSC at CS 3A was approximately 10 times higher than during S18, the SSC at the bottom was only two times higher. The highest SSC difference between the surface and the bottom was located at CS 3A, where the surface (0.1 and 0.2 depths) concentrations (~119 mg/l) were about five times higher than the bottom concentration (23 mg/l). Like turbidity, also the SSC decreased considerably between CS 3A and 4A. From CS 4A seawards, the SSC remained steady and below 31 mg/l within the water column.

Table 3. Pearson correlations between water quality parameters. The correlations between turbidity and SSC are bolded.

	S18 (n = 17)				W19 (n = 18)				A19 (n = 27)			
	Sal.	Temp.	SSC	Turb.	Sal.	Temp.	SSC	Turb.	Sal.	Temp.	SSC	Turb.
Sal.	–				–				–			
Temp.	-0.73	–			0.87	–			0.70	–		
SSC	-0.50	0.17	–		-0.72	-0.75	–		-0.98	-0.59	–	
Turb.	-0.86	0.49	**0.82**	–	-0.86	-0.82	**0.95**	–	-0.98	-0.59	**1.00**	–

During A19, turbidity was much higher at the CSs located closest to the river mouth (CSs 1–3A) than at the other CSs (Fig. 4). This time, turbidity was slightly higher at the bottom than at the surface at

CSs 1-2. At CS 3A, the bottom turbidity (167 NTU) became lower than at the surface, being approximately half of the surface value (311 NTU). Turbidity decreased seawards, especially after CS 3A, where the turbidity of the whole water column decreased dramatically. Surface turbidity remained slightly higher than bottom turbidity at CSs 3A–5B. From CS 6A seawards, the water column became more or less homogenous, having turbidity below 16 NTU. Once again, SSC had a similar pattern to turbidity (correlation 1.00) (Table 3). The highest SSCs were found at the CSs closest to the river mouth (CSs 1–3A). The bottom SSC was higher than the surface SSC, except in CS 3A, where the bottom was 94 mg/l lower than at the surface. The SSCs in CS 1 were more than 10 times higher than during S18. SSC decreased steadily towards the sea between CSs 1 and 3A. Before CS 4A, the SSCs at the whole water column decreased dramatically to the level of 21–25 mg/l, which was only a tenth and a fifth of the corresponding surface and bottom values of CS 3A, respectively. From CS 4A seawards, the surface and bottom SSCs became similar. During A19, the Secchi depth was less than 12 cm at CSs 1–4A (13.5 km from the river mouth) and started to increase rather steadily from CS 4A seawards (Fig. 4.). While during S18, the Secchi depth was 32 cm at CS 1, only 1 km from the river mouth, during A19, similar Secchi depth was located after CS 4A, ~14 from the river mouth.

5 Discussion

5.1 The behaviour of river plumes under different environmental conditions

Based on our results, we propose a conceptual model to explain the behaviour of river plumes and sediment transport in non-tidal brackish water estuaries (Fig. 7). During the low discharge of open water periods, river plumes do not extend far from the river mouth (Fig. 7, A). Observations during the low discharge period showed a typical example of estuarine condition and a vertically mixed water column, except at CSs 4A–7A, where the bottom was much colder than the surface. However, this phenomenon is likely to be related to the thermocline that suppresses the vertical mixing between the surface and bottom (Kullenberg and Jacobsen, 1981). Turbidity and SSC were highest and salinity lowest closest to the river mouth, as expected and the water column was vertically mixed at shallow depths (< 4 m). Observations did show a clear trend of decreasing turbidity towards offshore reflecting normal estuary conditions at low river discharge. The surface turbidity at CS 3A during S18 also less than a tenth than during either W19 and A19, and a Secchi depth of 77 cm was measured at CS 3A, indicating no river plume. While surface current was towards the river mouth, bottom current was towards the sea. This current pattern, also known as inverse estuary circulation, was most likely wind-driven due to the inshore-directed wind. It can thus be suggested that wind might induce inverse estuary circulation when there is no river input or tidal influence. Inverse estuary circulation have been previously found in estuaries where downwelling occurs at the estuary head due to strong evaporation and increased surface salinity (Wolanski, 1986). Both Kourafalou (2001) and Stumpf et al. (1993) have also shown that plume behaviour could be highly influenced by wind direction and speed. Our finding of the river plume behaviour at the low river discharge of the open water period is consistent with the study by Granskog et al. (2005a), also in a non-tidal brackish water estuary.

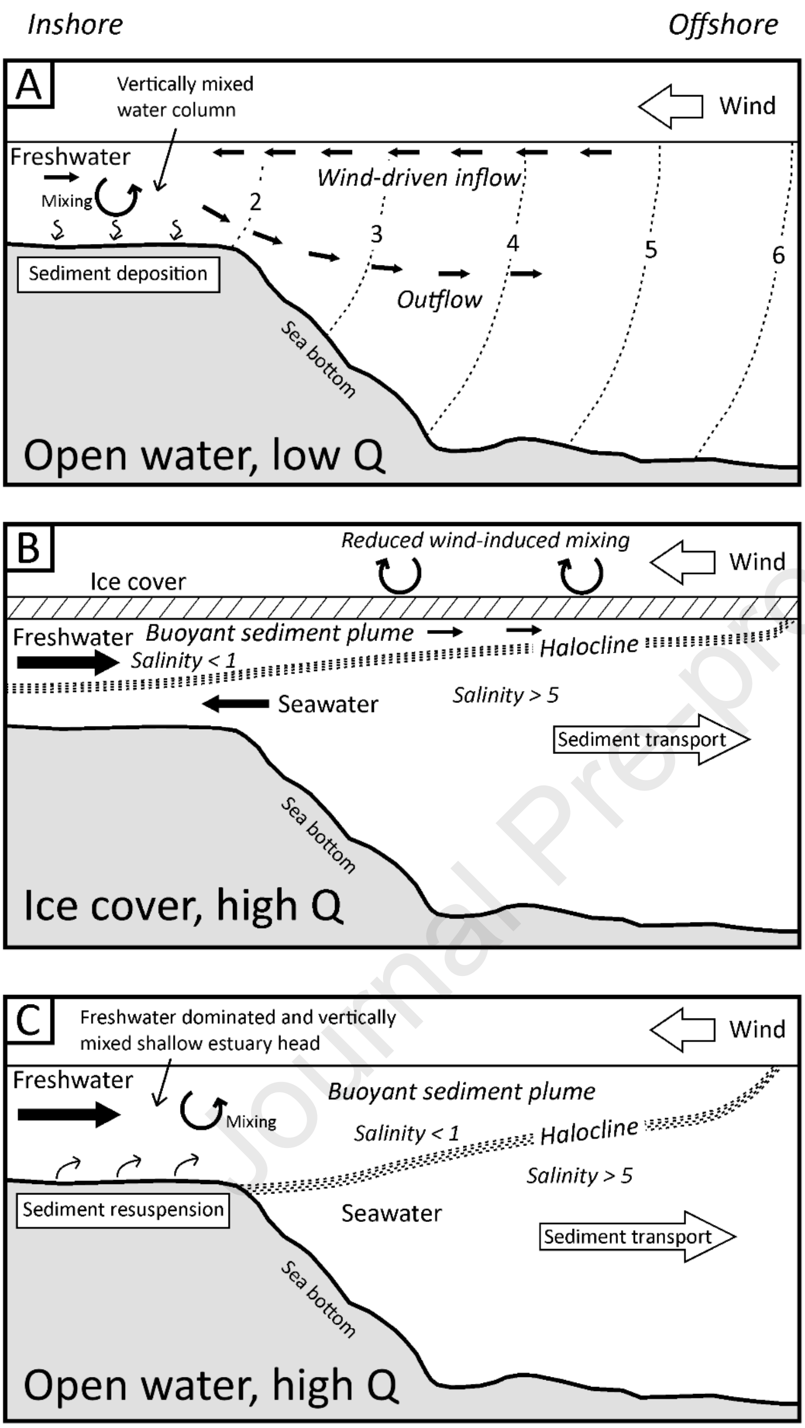

Figure 7. Conceptual model of the river plume development and sediment transport in non-tidal brackish water estuary. Dashed lines show isohalines.

In our study, higher river discharge was found to result in a more extended river plume in both ice-cover and open water conditions (Fig 8, B & C). During W19 (ice cover), an outflow-directed buoyant river plume developed. Clear differences in salinity, SSC and turbidity between the surface and bottom layers at CS 3A support the development of a buoyant river plume. In addition, the turbidity was considerably higher at 0.1 depth than at 0.8 depth or during open water conditions at low flow. For example, Kari et al. (2018) and Ingram and Larouche (1987) have also reported under-ice plume development in non-tidal and tidal estuaries respectively. Our current velocity measurements also support the development of buoyant river plume. Particularly at CS 3A, the water column was divided into two opposite flowing layers, where the fresh surface layer outflowed and the saline bottom layer inflowed. Pritchard (1952) described a similar two-layer current pattern in open water conditions caused by salinity stratification together with tidal influence. However, in our study, the current pattern was likely related to high river discharge, salinity stratification and reduced wind mixing by ice cover. The vertical extent of the river plume from the surface towards the sea bed diminished with the increased depth and distance from the river.

During A19, the river plume developed both in the whole water column and at the surface (Fig. 7, C). The estuary head, where the depth was less than 5 m, became freshwater dominated and vertically mixed. In addition, along the estuary, the water column was characterized by outflow, especially at the estuary head, indicating strong river influence. Similar behaviour have been previously found in tidal estuaries during ebb tides or under high river discharge when freshwater volume becomes larger than tidal volume (Mitchell et al. 2017; Orseau et al. 2017). High river discharge in relation to the shallow and narrow estuary head most likely caused the homogenous water column. At the estuary head, strong bottom current velocity may have caused sediment entrainment from the sea bottom, which may explain higher turbidity and SSC values near the bottom compared to surface. A buoyant river plume developed at the plume front, where the thickness of the plume was less than 2 m. While turbidity, SSC and salinity values at 0.1 depth did not clearly show the location of the buoyant river plume, the Secchi depths at CS 4A and CS 5B were only 10 cm and 50 cm, respectively, indicating a turbid surface plume. Stumpf et al. (1993) have also recorded similar variation in plume thickness between thicker inner plume and shallower outer plume in microtidal saline estuary. Different plume thickness in different parts of the estuary might be caused by variations of sea bed elevation and distance from the river mouth. Especially in a narrow and shallow estuary, the estuary head might become river-like (e.g. strong freshwater flow in the whole water column) during high river discharge periods, when the freshwater flow is strong enough to move salt wedges seawards. As the depth increases seawards, as in our study between CS 3A and CS 4A, the river plume may continue as a surface plume only, instead of mixing into the whole water column. For example, Granskog et al. (2005a) found that the plume thickness corresponded roughly to the channel depth at the mouth of the river. In addition, local smaller streams along the channel may provide more freshwater into the channels and thus influence plume thickness and size locally along the estuary.

5.2 Effect of salinity and wind on plume behaviour

In this study, even a small salinity difference (~5) between fresh river water and seawater was enough to create salinity stratification and reduce sediment mixing between the sediment rich freshwater and seawater. The stratification together with windless conditions maintained a buoyant river plume both in ice-cover and open water conditions. These results reflect those of Granskog et al. (2005a) and Kari et al. (2018), who also found formation of buoyant river plumes in non-tidal and weakly stratified (salinity difference less than five over the entire water column) ice-cover conditions. Similar under-ice plume development has also been found in tidal and saltier estuaries (Ingram and Larouche, 1987). Our data shows that buoyant river plumes may also develop in windless open water conditions under high river discharge, when wind-induced mixing is absent. During A19, buoyant river plume was found in the south channel where conditions were windless during the field measurements. Even though prevailing south-east directed (direction 100–200 degrees) winds with highest wind speed (6.5 m/s) were recorded one week and especially one day prior to the field campaign day in the south channel, a buoyant river plume together with stratified conditions and strong outflow pattern were found along the south channel. This finding is most likely to be related to high river flow when the volume of freshwater becomes higher than the volume of seawater and freshwater starts to dominate the estuary. Also currents controlled by high river flow may become strong and substitute wind induced currents under these conditions. Wind might, however, control the plume behaviour or even reduce the plume formation, as during S18. This result is in line with a previous study by Xia et al.

(2007), who found that strong winds tend to reduce the surface plume extend in the horizontal direction due to wind-induced mixing.

Contrary to salinity, we did not find that temperature difference between fresh river water and saline seawater contributes to plume development.

5.3 Sediment transport under different conditions

The results of this study show the similarities of SSC with turbidity and salinity values (Table 3). Thus, the transport of suspended sediment is highly dependent on river discharge, wind and stratification. During low river discharge open water periods, the suspended sediment most likely accumulates at the estuary head, where the water column is vertically mixed and river flow is too weak for creating outflow (Fig. 7, A). During high discharge ice-cover or open water conditions, the sediment transports much farther seawards due to the occurrence of buoyant river plumes and reduced wind-induced mixing (Fig. 7, B & C). Thus, sediment and particulate nutrients spread larger extent and mix with greater water masses than at shallow estuary head. This may cause spatiotemporal variation on sea bottom degradation, hypoxia or algal blooms in coastal waters. In addition, while in tidal estuaries the sediment transport is controlled by the combination of freshwater flow and tidal currents, in non-tidal estuaries the estuary current pattern and sediment transport are mainly controlled by freshwater flow and wind. Thus, sediment is mostly transported seawards only during high discharge periods, when fresh river water forms outflow along the estuary. In addition, strong freshwater outflow may cause resuspension in shallow estuary head where high current velocities reaches the sea bottom.

5.4. Limitations and future research

Our study combined water quality and current velocity measurements to examine river plume development. However, some limitations in the methodological approach were found during the study. First, water quality measurements should cover the whole water column, instead of discrete surface and bottom samples. For example, CTD (conductivity, temperature and depth) casts would give more detailed description of the entire water column and plume development. Despite the use of fast-moving motor boat, the collected data do not represent simultaneous situation of plume at each measurement location. In addition, the ADCP can adjust the cell size based on the water depth; it increased the cell sized up to 2 m in deeper locations, which limited the evaluation of buoyant water plume. Current measurements based on the Doppler effect, like ours, are insufficient in extremely clear waters because of the lack of backscattering from particles. This limits the measurements only in turbid waters. For example, in our study, the ADCP was unable to measure the bottom current in winter conditions due to lack of particles. In future studies, sedimentation-resuspension rates at non-tidal brackish water estuaries should be studied to understand the estuary sediment dynamics in more detail. Owing to very strong correlation (0.82– 1.00) between turbidity and SSC values, the sediment transport in Baltic Sea region could be studied with turbidity measurements only omitting laborious SSC calculations.

6 Conclusion

This study was designed to evaluate river plume behaviour and sediment transport under different conditions, including both open water and ice cover conditions. The study was performed in a non-tidal semi-enclosed brackish water estuary at the Archipelago Sea, Baltic Sea. The following conclusions can be drawn:

- Buoyant river plumes form in both ice-cover and windless open water conditions under high river discharge. Thus, the transport of suspended sediment is highly dependent on river discharge, wind conditions and stratification in non-tidal brackish water estuary.
- Ice cover contributes to the development of buoyant river plume by reducing wind-induced mixing.
- Even an extremely small salinity difference (~5) between fresh river water and seawater is strong enough to create a buoyant river plume in brackish water estuaries. This stratification reduces the mixing of suspended sediment between the fresh surface and saline bottom layer.
- River plumes may form simultaneously in time both in the whole water column and at the water surface during a high discharge period. While the shallow (depth < 5 m) estuary head is

dominated by a vertically homogenous plume, the plume front is buoyant. Thus, the depth of the river plume diminished with increased water depth and distance from the river mouth.

- Temperature differences between river water and seawater do not contribute to the development of buoyant river plumes or reduce the vertical mixing between the surface and bottom layers in regions where the sea and river waters are both more or less similar.
- Estuarine currents in a non-tidal estuary are controlled by wind and river discharge. High river discharge together with salinity stratification, that limits the mixing of surface and bottom waters, may induce positive estuary circulation. In addition, inshore-directed wind may reduce the development of river plumes and form inverse estuary circulation.
- In a brackish water non-tidal estuary, sediment plume development is largely controlled by river discharge variation. A plume develops under high river discharge, while during low river discharge, the plume is very limited in extent.

Acknowledgements

This study was funded by the Doctoral Programme in Biology, Geography and Geology at the University of Turku, the Strategic Research Council at the Academy of Finland (project “Competence Based Growth Through Integrated Disruptive Technologies of 3D Digitalization, Robotics, Geospatial Information and Image Processing/Computing – Point Cloud Ecosystem” [314312]) and Academy of Finland (project “InfraRiver” [296090]). The authors wish to thank Markus Katainen and Linnea Blåfield for assistance in fieldwork and the Finnish Environment Institute, Finnish Meteorological Institute, Economic Development, Transport and the Environment Centre and European Space Agency for data. The comments of two anonymous reviewers significantly improved the manuscript.

Bibliography

Beusen, A.H.W., Dekkers, A.L.M., Bouwman, A.F., Ludwig, W., Harrison, J., 2005. Estimation of global river transport of sediments and associated particulate C, N, and P. Global Biogeochem. Cycles 19. https://doi.org/10.1029/2005GB002453

Bonsdorff, E., Rönnberg, C., Aarnio, K., 2002. Some ecological properties in relation to eutrophication in the Baltic Sea. Hydrobiologia 475–476, 371–377. https://doi.org/10.1023/A:1020395526898

Chen, W.-B., Liu, W.-C., Hsu, M.-H., Hwang, C.-C., 2015. Modeling investigation of suspended sediment transport in a tidal estuary using a three-dimensional model. Appl. Math. Model. 39, 2570–2586. https://doi.org/10.1016/j.apm.2014.11.006

Coleman, J.M., 1988. Dynamic changes and processes in the Mississippi River delta. Geol. Soc. Am. Bull. 100, 999–1015. https://doi.org/10.1130/0016-7606(1988)100<0999

Cyrus, D.P., Blaber, S.J.M., 1992. Turbidity and salinity in a tropical northern Australian estuary and their influence on fish distribution. Estuar. Coast. Shelf Sci. 35, 545–563.

Erkkilä, A., Kalliola, R., 2004. Patterns and dynamics of coastal waters in multi-temporal satellite images: Support to water quality monitoring in the Archipelago Sea, Finland. Estuar. Coast. Shelf Sci. 60, 165–177. https://doi.org/10.1016/j.ecss.2003.11.024

Fernandez, J.M., Meunier, J.D., Ouillon, S., Moreton, B., Douillet, P., Grauby, O., 2017. Dynamics of suspended sediments during a dry season and their consequences on metal transportation in a Coral reef lagoon impacted by mining activities, New Caledonia. Water (Switzerland) 9. https://doi.org/10.3390/w9050338

Fonselius, S., 1969. Hydrography of the Baltic Deep basins III. Fish. Board Sweden, Ser. Hydrogr. 23, 97 pp.

Gilbert, M., Fortier, L., Ponton, D., Drolet, R., 1992. Feeding ecology of marine fish larvae across the Great Whale River plume in seasonally ice-covered southeastern Hudson Bay. Mar. Ecol. Prog. Ser. 84, 19–30. https://doi.org/10.3354/meps084019

Grabemann, I., Uncles, R.J., Krause, G., Stephens, J.A., 1997. Behaviour of turbidity maxima in the Tamar (U.K.) and Weser (F.R.G.) Estuaries. Estuar. Coast. Shelf Sci. 45, 235–246. https://doi.org/10.1006/ecss.1996.0178

Granskog, M.A., Ehn, J., Niemelä, M., 2005a. Characteristics and potential impacts of under-ice river plumes in the seasonally ice-covered Bothnian Bay (Baltic Sea). J. Mar. Syst. 53, 187–196. https://doi.org/10.1016/j.jmarsys.2004.06.005

Granskog, M.A., Kaartokallio, H., Thomas, D.N., Kuosa, H., 2005b. Influence of freshwater inflow on the inorganic nutrient and dissolved organic matter within coastal sea ice and underlying waters in the Gulf of Finland (Baltic Sea). Estuar. Coast. Shelf Sci. 65, 109–122. https://doi.org/10.1016/j.ecss.2005.05.011

Hänninen, J., Vuorinen, I., Helminen, H., Kirkkala, T., Lehtilä, K., 2000. Trends and gradients in nutrient concentrations and loading in the Archipelago Sea, northern Baltic, in 1970-1997. Estuar. Coast. Shelf Sci. 50, 153–171. https://doi.org/10.1006/ecss.1999.0568

HELCOM, 2009. Eutrophication in the Baltic Sea – An integrated thematic assessment of the effects of nutrient enrichment and eutrophication in the Baltic Sea region: Executive Summary. Balt. Sea Environ. Proc. No. 115A.

Hir, P. Le, Ficht, A., Jacinto, R.S., Lesueur, P., Dupont, J.P., Lafite, R., Brenon, I., Thouvenin, B., Cugier, P., 2001. Fine sediment transport and accumulations at the mouth of the Seine estuary (France). Estuaries 24, 950–963. https://doi.org/10.2307/1353009

Ingram, R.G., Larouche, P., 1987. Variability of an under-ice river plume in Hudson Bay. J. Geophys. Res. Ocean. 92, 9541–9547. https://doi.org/10.1029/JC092iC09p09541

Ingram, R.G., Wang, J., Lin, C., Legendre, L., Fortier, L., 1996. Impact of freshwater on a subarctic coastal ecosystem under seasonal sea ice (southeastern Hudson Bay, Canada). I. Interannual variability and predicted global warming influence on river plume dynamics and sea ice. J. Mar. Syst. 7, 221–231. https://doi.org/10.1016/0924-7963(95)00006-2

Kari, E., Merkouriadi, I., Walve, J., Leppäranta, M., Kratzer, S., 2018. Development of under-ice stratification in Himmerfjärden bay, North-Western Baltic proper, and their effect on the phytoplankton spring bloom. J. Mar. Syst. 186, 85–95. https://doi.org/10.1016/j.jmarsys.2018.06.004

Kourafalou, V.H., 2001. River plume development in semi-enclosed Mediterranean regions: North Adriatic Sea and Northwestern Aegean Sea. J. Mar. Syst. 30, 181–205. https://doi.org/10.1016/S0924-7963(01)00058-6

Kullenberg, G., Jacobsen, T.S., 1981. The Baltic Sea: an outline of its physical oceanography. Mar. Pollut. Bull. 12, 183–186. https://doi.org/10.1016/0025-326X(81)90168-5

Kuzyk, Z.A., Macdonald, R.W., Granskog, M.A., Scharien, R.K., Galley, R.J., Michel, C., Barber, D., Stern, G., 2008. Sea ice, hydrological, and biological processes in the Churchill River estuary region, Hudson Bay. Estuar. Coast. Shelf Sci. 77, 369–384. https://doi.org/10.1016/j.ecss.2007.09.030

MacCready, P., Banas, N.S., Hickey, B.M., Dever, E.P., Liu, Y., 2009. A model study of tide- and wind-induced mixing in the Columbia River Estuary and plume. Cont. Shelf Res. 29, 278–291. https://doi.org/10.1016/j.csr.2008.03.015

Macdonald, R.W., Carmack, E.C., 1991. The role of large□scale under□ice topography in separating estuary and ocean on an arctic shelf. Atmos. - Ocean 29, 37–53. https://doi.org/10.1080/07055900.1991.9649391

Mitchell, S.B., Green, M.O., MacDonald, I.T., Pritchard, M., 2017. Field studies of estuarine turbidity under different freshwater flow conditions, Kaipara River, New Zealand. Estuar. Coast. Shelf Sci. 198, 542–554. https://doi.org/10.1016/j.ecss.2016.06.009

Molleri, G.S.F., Novo, E.M.L. d. M., Kampel, M., 2010. Space-time variability of the Amazon River plume based on satellite ocean color. Cont. Shelf Res. 30, 342–352. https://doi.org/10.1016/j.csr.2009.11.015

Orseau, S., Lesourd, S., Huybrechts, N., Gardel, A., 2017. Hydro-sedimentary processes of a shallow tropical estuary under Amazon influence. The Mahury Estuary, French Guiana. Estuar. Coast. Shelf Sci. 189, 252–266. https://doi.org/10.1016/j.ecss.2017.01.011

Pedersen, T.M., Gallegos, C.L., Nielsen, S.L., 2012. Influence of near-bottom re-suspended sediment on benthic light availability. Estuar. Coast. Shelf Sci. 106, 93–101. https://doi.org/10.1016/j.ecss.2012.04.027

Pritchard, D.., 1952. Salinity distribution and circulation in the Chesapeake Bay estuarine system. J. Mar. Res. 11(2), 106–123.

Pritchard, M., Huntley, D.A., 2006. A simplified energy and mixing budget for a small river plume discharge. J. Geophys. Res. Ocean. 111, 1–11. https://doi.org/10.1029/2005JC002984

Ren, J., Wu, J., 2014. Sediment trapping by haloclines of a river plume in the Pearl River Estuary. Cont. Shelf Res. 82, 1–8. https://doi.org/10.1016/j.csr.2014.03.016

Restrepo, J.C., Schrottke, K., Traini, C., Bartholomae, A., Ospino, S., Ortíz, J.C., Otero, L., Orejarena, A., 2018. Estuarine and sediment dynamics in a microtidal tropical estuary of high fluvial discharge: Magdalena River (Colombia, South America). Mar. Geol. 398, 86–98. https://doi.org/10.1016/j.margeo.2017.12.008

Stumpf, R.P., Gelfenbaum, G., Pennock, J.R., 1993. Wind and tidal forcing of a buoyant plume, Mobile Bay, Alabama. Cont. Shelf Res. 13, 1281–1301. https://doi.org/10.1016/0278-4343(93)90053-Z

Uncles, R.J., Stephens, J.A., Law, D.J., 2006. Turbidity maximum in the macrotidal, highly turbid Humber Estuary, UK: Flocs, fluid mud, stationary suspensions and tidal bores. Estuar. Coast. Shelf Sci. 67, 30–52. https://doi.org/10.1016/j.ecss.2005.10.013

Van Maren, D.S., Hoekstra, P., 2004. Seasonal variation of hydrodynamics and sediment dynamics in a shallow subtropical estuary: The Ba Lat River, Vietnam. Estuar. Coast. Shelf Sci. 60, 529–540. https://doi.org/10.1016/j.ecss.2004.02.011

Walker, N.D., Wiseman, W.J., Rouse, L.J., Babin, A., 2005. Effects of River Discharge, Wind Stress, and Slope Eddies on Circulation and the Satellite-Observed Structure of the Mississippi River Plume. J. Coast. Res. 216, 1228–1244. https://doi.org/10.2112/04-0347.1

Wolanski, E., 1986. An evaporation-driven salinity maximum zone in Australian tropical estuaries. Estuar. Coast. Shelf Sci. 22, 415–424. https://doi.org/10.1016/0272-7714(86)90065-X

Wu, J., Liu, J.T., Wang, X., 2012. Sediment trapping of turbidity maxima in the Changjiang Estuary. Mar. Geol. 303–306, 14–25. https://doi.org/10.1016/j.margeo.2012.02.011

Xia, M., Xie, L., Pietrafesa, L.J., 2007. Modeling of the cape fear river estuary plume. Estuaries and Coasts 30, 698–709. https://doi.org/10.1007/BF02841966

YSI Professional Plus (Pro Plus) Multiparameter Instrument. URL. https://www.ysi.com/proplus. Accessed date: 14 June 2020.

Yuan, D., Yang, D., 2001. Status of persistent organic pollutants in the sediment from several estuaries in China. Environ. Pollut. 114, 101–111. https://doi.org/10.1016/S0269-7491(00)00200-1

	S18 (Summer 2018)		W19 (Winter 2019)		A19 (Autumn 2019)	
Condition	Open water		Ice cover		Open water	
Date	27.6	28.6	20.3	21.3	14.11	15.11
Channel	North (B)	South (A)	North (B)	South (A)	North (B)	South (A)
Number of water quality measurements	12	19	15	15	18	30
Water sampling depth (% of the site depth)	20/80	20/80	10/20/80	10/20/80	10/20/80	10/20/80
Number of flow measurements	6	9	5	5	6	9
River discharge	Derived from SYKE					
River turbidity	Derived from ELY					
Wind direction and speed	Derived from FMI					

	S18		W19		A19	
Date	27.6	28.6	20.3	21.3	14.11	15.11
Channel	North (B)	South (A)	North (B)	South (A)	North (B)	South (A)
Daily river discharge (m^3/s)	0.23	0.2	39.5	27.5	40	31.2
Daily river turbidity (NTU)	33	33	353	287	548	499
Wind direction (deg)	227–277	213–247	206–257	177–244	174–178	11–112
Wind speed (m/s)	3.4–4.3	5.5–8.8	3.8–8.0	2.9–6.2	7.5–8.3	1.7–2.1

	S18 (n = 17)				W19 (n = 18)				A19 (n = 27)			
	Sal.	Temp.	SSC	Turb.	Sal.	Temp.	SSC	Turb.	Sal.	Temp.	SSC	Turb.
Sal.	–				–				–			
Temp.	-0.73	–			0.87	–			0.70	–		
SSC	-0.50	0.17	–		-0.72	-0.75	–		-0.98	-0.59	–	
Turb.	-0.86	0.49	**0.82**	–	-0.86	-0.82	**0.95**	–	-0.98	-0.59	**1.00**	–

Highlights:

- Buoyant river plumes form in both ice-covered and open water conditions
- Buoyant river plumes form even in conditions of low salinity stratification
- Low salinity stratification reduces sediment mixing within water column
- Small water temperature differences do not contribute the behaviour of river plumes

Declaration of interests

☒ The authors declare that they have no known competing financial interests or personal relationships that could have appeared to influence the work reported in this paper.

☐The authors declare the following financial interests/personal relationships which may be considered as potential competing interests: